EAI Endorsed Transactions
on Energy Web

Research Article EAI.EU

Construction of a Fast Monitoring System for Electric Energy Equipment Status Based on Data Mining

Fusheng Wei[1], Xue Li[1], Weiwen Chen[1], Zhaokai Liang[2,*], Zhaopeng Huang[3]

[1]Guandong Power Grid Co., Ltd., Guangzhou, 510000, China
[2]Guangzhou Power Supply Bureau of Guangdong Power Grid Co., Ltd., Guangzhou, 510000, China
[3]Foshan Power Supply Bureau of Guangdong Power Grid Co., Ltd., Foshan, 528000, China

Abstract

In modern power system operation, it is crucial to achieve fast and accurate monitoring of the electrical equipment status. To achieve this fast and accurate detection, this study proposes a generative adversarial network that combines edge features to amplify and recognize infrared images of devices, aiming to improve the model's training effect. This model extracted edge features from infrared images to eliminate background noise in infrared images to achieve the goal of improving the accurate monitoring of the status of electrical equipment. The results showed that on the balanced dataset, the recognition accuracy of the model could reach about 96%, and the recognition effect of the model was relatively stable. On imbalanced datasets, the highest model recognition accuracy was around 89%, and the model recognition accuracy fluctuated greatly. The constructed model effectively improves the accuracy of monitoring the operating status of electric energy equipment, achieving fast and accurate monitoring of this state. This study can achieve rapid monitoring of the operating status of electric energy equipment, effectively reducing the operation and maintenance costs of the power system.

Keywords: Data mining; Electric energy equipment; Status monitoring; Edge perception; Generative adversarial network.

Received on 23 04 2024, accepted on 30 08 2024, published on 20 12 2024

doi: 10.4108/ew.5869

*Corresponding author. Email: lzk55699@163.com

1. Introduction

In the context of digital transformation, the power industry is urgently in need of efficient monitoring systems to ensure the safety and stable operation of power equipment [1-2]. The electrical Equipment Status Monitoring (ESM) is a technology for monitoring the main equipment in the power system. During the operation of Electrical Energy Equipment (3E), temperature changes may occur due to the electric heating effect. The status detection of electric energy equipment is to monitor the temperature status of the equipment to reflect its operating status. Timely and accurate ESM can ensure the safety of system operation. Data mining technology, as a product of the intelligent era, is particularly crucial in the monitoring of the status of power equipment. It can analyze a large amount of data generated by equipment to predict potential failures and performance degradation of the equipment [3-4]. However, due to the complexity of the operation of 3E and the enormous amount of data generated, as well as the changing characteristics, developing a fast and accurate monitoring system to adapt to rapidly changing industrial demands remains a technical challenge [5-6]. To improve the efficiency and accuracy of state detection for electric energy equipment, this study designs a device state detection method based on data mining technology.

This study innovatively proposes a monitoring system framework that integrates data mining algorithms, and specifically optimizes the operational characteristics and data attributes of power equipment. The research results provide an effective means to improve the response speed and accuracy of power equipment monitoring, and are of great significance for the future intelligent management and preventive maintenance of power equipment.

This study will be conducted from four aspects. Firstly, it will provide an overview of the current research status of power ESM and Infrared Image (IFI) data mining. Secondly, the research on power ESM combines Edge Feature Monitoring (EFM) and Generative Adversarial Networks (GAN). The third is the experimental analysis of the electrical ESM network, and finally the summary of the research content.

2. Related works

The electrical ESM is meaningful for the safe Operation of the Power System (O-PS), and effective status monitoring can help workers better maintain the power system. Jin X et al. gave an integrated method to detect anomalies and diagnose faults to extract health related information from monitoring and data collection of wind turbine conditions. This method could detect anomalies and diagnose corresponding faulty components before the wind turbine was shut down for maintenance [7]. Zhao et al. compared various state monitoring methods for DC link capacitors to improve the reliability of systems. It introduced the design process of capacitor common mode, summarized the main principles of capacitor parameter estimation, and derived various possible common mode schemes. At last, application suggestions were proposed [8]. To ensure the long-term reliability and extend the lifespan of solar photovoltaic systems, it is necessary to optimize their monitoring, operation, and maintenance. Di Lorenzo G et al. proposed a new remote monitoring technology that reduces or eliminates duplicate component failures by investigating and resolving faults in photovoltaic systems. These technologies contributed to improving fault reporting and corrective action systems, enhancing the reliability and availability of photovoltaic systems [9]. Wang B et al. proposed an automatic diagnosis method built on infrared insulator image instance segmentation and temperature analysis to improve the efficiency of on-site diagnosis of substation insulators. This method had high recognition accuracy and computational speed, and had a huge potential practicality in the field of diagnosing power equipment [10].

GAN has a wide range of applications in various image processing fields and is an excellent IFI processing algorithm. Liu M et al. proposed an overview of GANs to improve their performance in image and video synthesis tasks, with a particular focus on applications of visual synthesis. GAN could generate high-resolution realistic images and videos, leading to the creation of many new Apps in content creation [11]. Maeda H proposed using generative models to generate Road Damage (RD) images to address the insufficient data for RD detection in infrastructure inspections. It combined the gradually growing GAN with Poisson mixture, artificially generated RD images, and added them to the training data to improve the RD detection accuracy. When the number of original images was small and relatively large, the synthesized images were measured at 5% and 2%, respectively, significantly improving the detection accuracy [12]. Pavan Kumar M R et al. proposed the use of deep neural networks, including variational auto-encoders, auto-regressive models, and GANs, to solve the problem of high-dimensional data generation. GANs had received widespread attention in generating high-quality images and data augmentation. These methods could generate high-quality data required for various tasks [13]. Zhao B et al. proposed a GAN-based infrared small target detection mode to solve the existed related problems. This method automatically learned target features through a GAN model and reconstructed the target using a U-Net generator. The five-layer discriminator and L2 loss could enhance the data fitting ability of the generator. Numerous experiments had shown that this method performed well on various backgrounds and targets, significantly improving the IoU value of detection results [14]. Jiang Y et al. proposed a CT image synthesis method based on conditional GAN to handle the matter of insufficient CT imaging data of COVID-19. This approach could generate

high-quality and realistic CT images of COVID-19 for medical imaging tasks based on deep learning. This method was superior to other advanced image synthesis ways and was expected to be used in various machine learning applications [15].

In summary, the electrical ESM is essential for the safety and stability of the O-PS. However, the current effectiveness of electrical ESM is poor and cannot accurately provide feedback on its status. Therefore, this study proposes to use infrared monitoring technology to detect 3E, and use EOGAN technology to analyze and process the images of 3E.

3. Combining EFM and GAN for power equipment status monitoring

The electrical ESM helps workers determine the O-PS, which is crucial for its safety and stability. This study focuses on the ESM from two aspects. The first part is the EFM analysis of power equipment, and the second part is the exploration of Infrared Image Generation (IIG) of power equipment grounded on EOGAN.

3.1. EFM of electrical energy equipment

The edge features of power equipment can guide the IIG of power equipment. Using device edge features as prior knowledge for weakly supervised learning can finish the guidance of IIG [16]. EFM is divided into four basic steps: scale normalization and grayscale, Gaussian filtering denoising, mathematical morphology processing, and edge detection. The original IFIs have differences in size due to different sources. The research relies on real-time detection data as the data source, using detection data from the Supervisory Control and Data Acquisition (SCADA) system as algorithm input. There are differences between the image data collected by SCADA. Inconsistent dimensions can cause obstacles in image processing and analysis, therefore, scale normalization of the image is necessary before EFM. Compared to visible light images, IFIs lack significant contrast, resulting in unclear boundaries between the device area and the background area, which affects subsequent image analysis and feature extraction work. Grayscale conversion can highlight the brightness information of an image, ignore color information, and increase contrast in the image. The calculation formula for converting IFIs to grayscale images is equation (1).

$$Grey = R*0.299 + G*0.587 + B*0.114 \quad (1)$$

In equation (1), $Grey$ represents the grayscale value of pixels in the IFI. R, G, B are the values of red, green, and blue colors in the image. Gaussian filtering is one of the most commonly used smoothing techniques in the field of image processing, which has excellent effects in eliminating Gaussian noise and can maintain the overall structure of the image, reducing excessive blurring. The Gaussian filtering operation is equation (2).

$$I_\sigma = I_{Gray} * G_\sigma \quad (2)$$

In equation (2), I_σ means the denoised image. I_{Gray} is the original grayscale image. G represents a 2D Gaussian kernel. σ denotes the standard deviation, and G_σ can be defined as equation (3).

$$G_\sigma = \frac{1}{2\pi\sigma^2} e^{-\left(x^2-y^2\right)/2\sigma^2} \quad (3)$$

In equation (3), x and y represent the Horizontal and Vertical (H/V) coordinates of pixels. The grayscale processing and denoising of IFIs are shown in Figure 1.

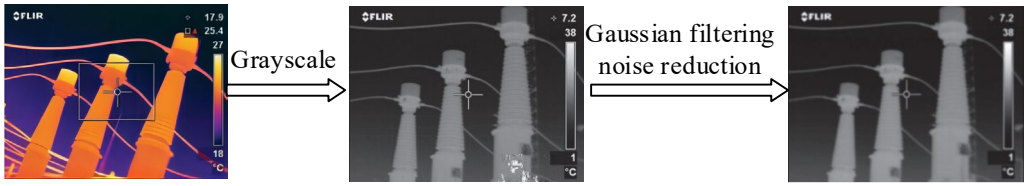

Figure 1. Gray measurement and noise reduction of IFIs

After size normalization, grayscale transformation, and Gaussian filtering denoising, the overall image is relatively rough and contains irrelevant objects. Unrelated objects can reduce the feature extraction ability of edge detection. Mathematical morphology is a vital branch in digital image processing, widely utilized in tasks such as image noise reduction, contour extraction, morphology measurement, image segmentation, and image

reconstruction [17]. The basic operations in mathematical morphology are dilation and erosion, which expand objects by adding pixels to the image. The corrosion operation removes pixels near the edge of the object, which can be used to eliminate small noise and small protrusions, and it also makes the object contour more delicate. The input image can be viewed as a function that maps Euclidean space E to a real number. If the function of the input image is assumed to be $f(x,y)$. $b(x,y)$ is the operator, then the image dilation operation is defined as equation (4).

$$(f \oplus b)(x) = \sup_{y \in E}\left[f(y) + b(x-y)\right] \tag{4}$$

In equation (4), $\sup$ represents the minimum upper bound. The corrosion operation is equation (5).

$$(f \oplus b)(x) = \inf_{y \in E}\left[f(y) - b(x-y)\right] \tag{5}$$

In equation (5), it represents the maximum lower bound of $\inf$. When using this method to process images, it is necessary to open the image, that is, first to corrode and then expand as shown in equation (6).

$$f \circ b = (f \ominus b) \oplus b. \tag{6}$$

After mathematical morphology processing, edge detection processing can be performed on the IFI of the device. This study uses the Sobel algorithm for edge detection, which can identify the boundaries of regions in the image and detect edges by calculating the spatial gradient of image grayscale. The Sobel algorithm uses two 3x3 convolution kernels to perform H/V gradient approximation calculations on the image, respectively. After calculating the H/V gradients of the image using convolutional kernels, the two gradients need to be merged to obtain a total gradient amplitude and direction. After obtaining the gradient amplitude, comparing it with the preset or adaptively calculated threshold to determine whether the pixel is located at the edge. If the gradient amplitude is higher than the threshold, the pixel is marked as an edge. The mathematical morphology processing and edge detection processing are shown in Figure 2.

Figure 2. Mathematical morphology and edge detection and treatment

3.2. EOGAN-based infrared image generation for power equipment

GAN is a deep learning model used for unsupervised learning tasks, whose core lies in the adversarial game dynamics between generator G and discriminator D [18-19]. The basic responsibility of generator G is to learn how to produce realistic data. G starts from a random noise distribution and gradually learns mapping relationships to generate samples that match the true data distribution. During the training process, the generator continuously tries to improve its camouflage ability, so that the generated data can deceive the discriminator. Discriminator D is a binary classification network whose task is to distinguish whether the input samples are "real". It accepts synthesized samples from the generator and samples from real datasets, and attempts to accurately determine whether these samples are from the real distribution or the generator. The discriminator continuously improves its discriminative ability and continuously identifies the generated samples from the generator. This adversarial process is trained through backpropagation and gradient descent. The network parameters of the generator and discriminator are constantly updated, with the aim of maximizing the deception ability of the generator and the discriminative ability of the discriminator, respectively. As the training progresses, the fake samples generated by the generator will become increasingly difficult to distinguish from the real samples, and the judgment task of the discriminator will also become more and more difficult. The function of GAN is equation (7).

$$\min_G \max_D V(D,G) = \min_G \max_D \left(\mathrm{E}_{z\sim p_z(z)} \log D(x) + \mathrm{E}_{z\sim p_z(z)} \log\left(1 - D(G(z))\right)\right) \tag{7}$$

In equation (7), z represents the noise vector. p_r represents the prior distribution of the sample. $D(x)$

and $D(G(z))$ are the evaluation of the discriminator on real samples (RS) and the samples generated by the generator (GS) using noise. In an ideal state, the training of GAN will end at a Nash equilibrium point, where the GS cannot be distinguished from the RS, and the discriminator can only make random guesses. The data generation process of GAN cannot be controlled, and when using this network for IIG and recognition, the complexity of image background information may cause GAN to not converge. Edge detection can extract edge features from IFIs and eliminate noise in background information [20]. Therefore, this study proposes to combine edge detection with GAN to obtain EDGAN. The training process of this network is Figure 3.

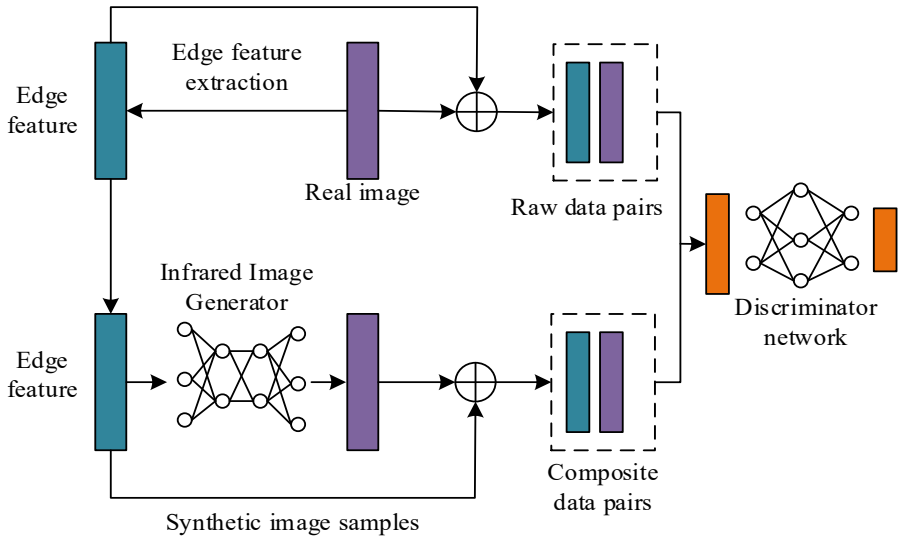

Figure 3. The training process of EDGAN

Conditional features are added to EDGAN; therefore, the network data is a supervised learning process. In the GAN of IFI processing, the original IFI x and the extracted edge features y are combined into the original data pair to guide model training. Generator G receives noise z and edge y, producing a realistic infrared composite image $G(x|y)$. These composite images are fused with edge features y to form composite data pairs, which together serve as training inputs for discriminator D. In adversarial training, G's goal is to generate images that are hard to distinguish by D, while D strives to distinguish between true and false, competing with each other to ultimately generate high-quality IFIs and capture detailed edge features, and supplement and enhance the sample data during the training process. In EDGAN, the loss function $L_{EDGAN}^{(D)}\left(\theta^{(G)},\theta^{(D)}\right)$ of discriminator D is equation (8).

$$L_{EDGAN}^{(D)}\left(\theta^{(G)},\theta^{(D)}\right)=\mathrm{E}_{x-p_{data}}\log D(x|y)-\mathrm{E}_{z}\log\left(1-D\left(G(z|y)\right)\right) \quad (8)$$

In equation (8), $D(x|y)$ and $D\left(G(z|y)\right)$ are the evaluation of the discriminator on real IFIs and synthesized IFI. $\theta^{(G)}$ represents the discriminator parameter. $\theta^{(D)}$ represents the generator parameter. In each training session, the discriminator parameters are updated by reducing the random gradient. The generator loss function is equation (9).

$$L_{EDGAN}^{(G)}\left(\theta^{(G)},\theta^{(D)}\right)=-\mathrm{E}_{z}\log D\left(G(z|y)\right) \quad (9)$$

To further optimize the generation results of the generator, this study adds an L1 distance loss function in equation (9), as shown in equation (10).

$$L_{L1}(G)=\mathrm{E}_{x,y,z}\left\|x-G(y,z)\right\|_{1.} \quad (10)$$

After adding the loss function, the generator needs to pass the detection of the discriminator and make the generated image closer to the real image. After that, the generator's loss function can be expressed as equation (11).

$$L_{EDGAN}^{(G)}\left(\theta^{(G)},\theta^{(D)}\right)=-\mathrm{E}_{z}\log D\left(G(z|y)\right)+\lambda\mathrm{E}_{x,y,z}\left\|x-G(y,z)\right\|_{1.} \quad (11)$$

In equation (11), λ represents the loss function

parameter. After training, the EDGAN can generate realistic and key information preserved IFIs of electrical equipment based on edge features. The generation process is Figure 4.

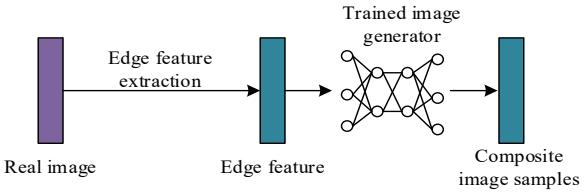

Figure 4. The training process of EDGAN

The IIG results of electrical equipment generated by the EDGAN model can be used to monitor the operating status of electrical equipment through IFI recognition technology. The designed equipment operation status monitoring is to transform equipment identification and fault detection problems into data-driven classification problems. Convolutional Neural Networks (CNN) are commonly utilized in image feature extraction. Therefore, this study applies CNN for deep feature extraction in device status monitoring, and then uses transfer learning method to perfect the model's training and learning speed. The designed electrical ESM framework is Figure 5.

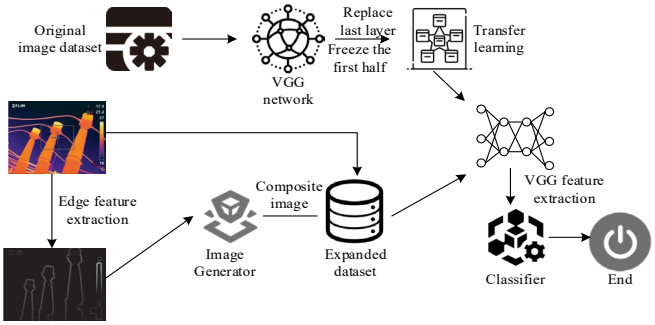

Figure 5. Electrical ESM framework

In this framework, VGG16 is used as the feature extraction network, and transfer learning and VGG16 model are used to recognize and detect faults in real IFIs and synthetic images. The input image size is 224*224, and after mining and feature extraction, a feature vector with a size of 7*7*512 is generated. By using a deep learning framework, power equipment identification and fault detection are transformed into classification problems. Softmax classifier is a commonly used classification model. This function converts a set of real numbers into a probability distribution, so that each real value corresponds to a probability value. If the training set function is assumed to be equation (12).

$$h_\theta\left(x^{(i)}\right)=\begin{bmatrix} p\left(y^{(i)}=1\middle|x^{(i)};\theta\right) \\ p\left(y^{(i)}=2\middle|x^{(i)};\theta\right) \\ \vdots \\ p\left(y^{(i)}=k\middle|x^{(i)};\theta\right) \end{bmatrix} \quad (12)$$

In equation (12), $h_\theta\left(x^{(i)}\right)$ represents the training set function. k represents the classification category. According to maximum likelihood estimation, the loss function of Softmax classifier is equation (13).

$$J(\theta)=\frac{1}{n}\left[\sum_{i=1}^{n}\sum_{j=1}^{k}1\left\{y^{(i)}=j\right\}\log\frac{e^{\theta_j^1 x^{(i)}}}{\sum_{i=1}^{k}e^{\theta_l^T x^{(i)}}}\right] \quad (13)$$

In equation (13), $y^{(i)}=j$ is the judgment of its true or false proposition. $J(\theta)$ represents the Softmax loss function. n is the quantity of samples. The overall architecture of the power ESM method based on the EDGAN model is divided into three stages: edge feature extraction, IIG of power equipment, and power ESM. The overall architecture is Figure 6.

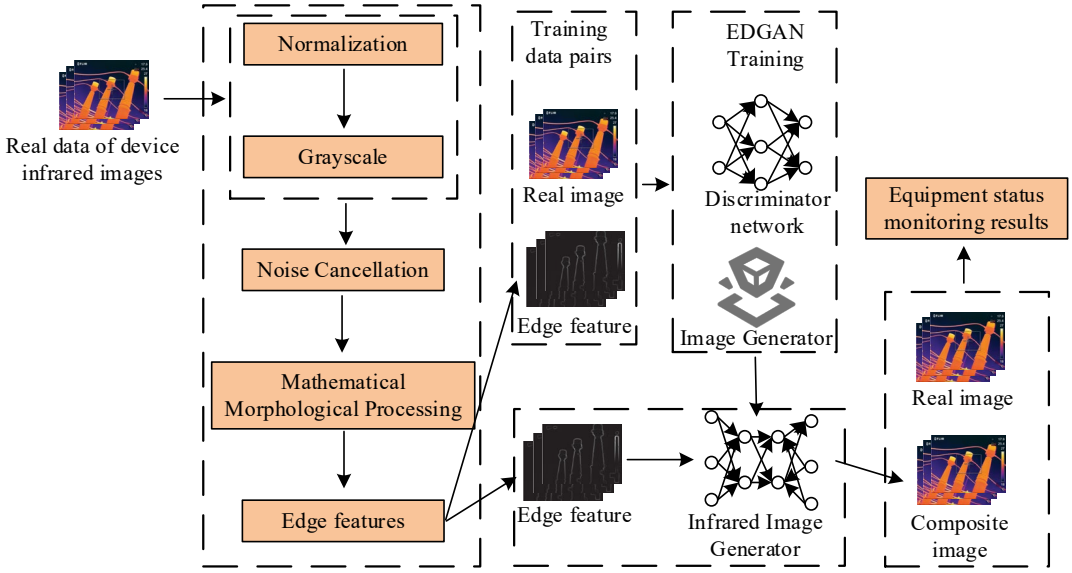

Figure 6. Overall framework of IFI amplification of electrical equipment based on EDGAN

When monitoring the operating status of 3E, it is not only needed to identify the status of O-PS, but also to perform semantic segmentation of equipment faults. Gated recurrent neural network is an effective feature mining model. This study proposes to use this model to conduct data mining on equipment fault status and analyze the changes in the basic image of equipment under the operation status of equipment faults. When repairing electrical equipment, it is necessary to continuously capture infrared images of the equipment. After capturing the equipment images, the equipment's infrared images will be directly uploaded to the image processing center. The image processing center processes the infrared images of the equipment based on the research and design model, and then uploads the data. The number of electric energy devices is relatively small, and the detection time for each device is long. The algorithm processing module has enough time to complete image processing and diagnostic work.

4. Analysis of the monitoring effect of 3E status based on EOGAN

In Chapter 2, a method for monitoring the 3E status based on EOGAN was proposed. To verify the feasibility of this method, experimental analysis was conducted in Chapter 3. Chapter 3 has two parts. Part 1 is the analysis of model simulation experiments, and Part 2 analyzes the actual application results of the model.

4.1. Model simulation experiment analysis

The experiment used IFIs from daily inspections of X City Power Supply Bureau as experimental data. The experimental image resolution was 640 × 480, and the thermal sensitivity was 0.06 ℃. Among them, there were 1200 images in the normal operating state and 900 images in the faulty operating state. The dataset for normal operation includes five types of electrical equipment, namely lightning arresters, circuit breakers, current transformers, voltage transformers, and Y-shaped circuit breakers. Random Forest (RF) and Support Vector Machine (SVM) are two common classification algorithms. To compare the impact of different classifiers on the final results, an unbalanced dataset was constructed with 1900 data samples, and the performance of three classifiers under different sample amplifications was analyzed. The result is displayed in Figure 7.

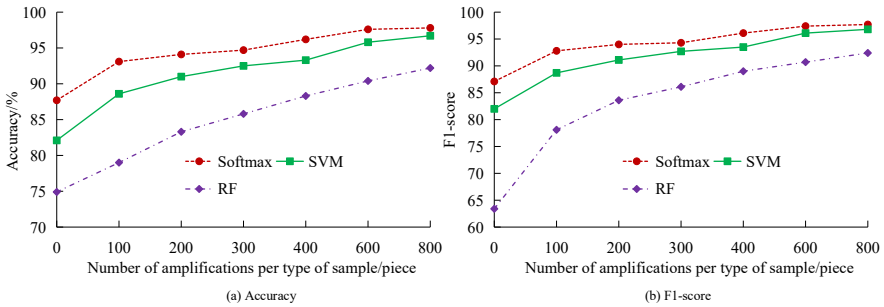

Figure 7. Changes in performance under the amplification of the different samples

Figure 7 (a) shows the recognition accuracy of different classifiers under different sample amplifications. As the sample size increased, the recognition accuracy of all three classifications continued to increase. When each sample was amplified to 800, the recognition accuracy of softmax was 97.8%, SVM was 96.7%, and RF was 92.2%. Figure 7 (b) shows the F1 scores of different classifiers under different sample amplifications. The changes in F1 scores for the three classifications were similar to the changes in recognition accuracy, both increasing with the expansion of samples in each category. When each class of samples was amplified to 800, the F1 score of softmax increased to 97.7 points, while the scores of the other two classifiers were lower than softmax. With the continuous increase of sample data, the accuracy and F1 score of the model are also increasing. The research designed model is recognized for maintaining high robustness and scalability when dealing with constantly expanding data samples. To validate the effect of imbalanced datasets on the classification accuracy, both the balanced and an imbalanced dataset were constructed, and the accuracy and loss of the model on the two datasets were compared, as shown in Figure 8.

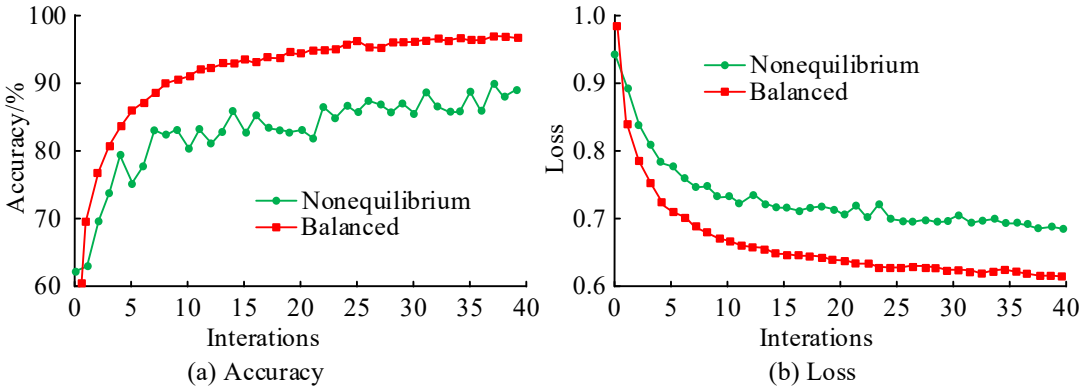

Figure 8. Effect of different datasets on the model training results

Figure 8 (a) shows the recognition accuracy on two datasets. As the iterations increased, the recognition accuracy on both datasets continued to increase. On a balanced dataset, the recognition accuracy could reach around 96%, and the recognition performance was relatively stable. On imbalanced datasets, the highest model recognition accuracy was around 89%, and the model recognition accuracy fluctuated greatly. Figure 8 (b) shows the comparison of model loss on two datasets. The model could effectively converge on both datasets. After the model converged on a balanced dataset, the damage degree could be reduced to below 0.2, while on an imbalanced dataset, the loss degree remains around 0.4. To further analyze the impact of two types of data on the model, the model identification confusion matrix was plotted on both datasets, as shown in Figure 9.

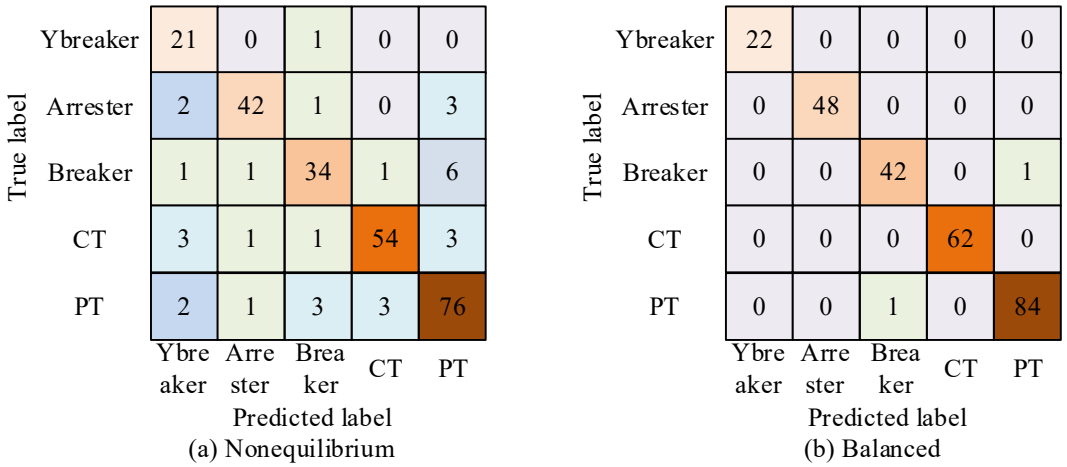

Figure 9. Model identification confusion matrix under different datasets

Figures 9 (a) and (b) show the identification confusion matrices on imbalanced and balanced datasets. By observing the confusion matrix, many circuit breakers and power transformers were incorrectly identified as voltage transformers (trained on the imbalanced dataset). The model (balanced dataset) using the EDGAN method largely avoided this problem. EDGAN enhanced minority class samples through GAN, increasing their weights during the training process, thereby balancing the samples from different categories in the dataset, enabling the model to better learn the features of each category and classify them more accurately. This study also analyzed the confusion matrix of the model for fault detection of electrical equipment under two datasets, as shown in Figure 10.

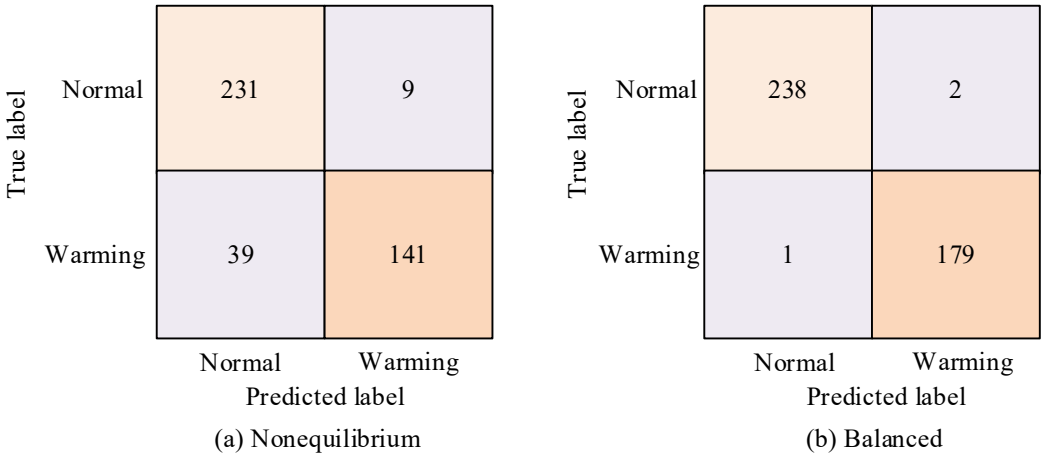

Figure 10. Failure detection confusion matrix under different datasets

Figures 10 (a) and 10 (b) show the fault detection confusion matrices for imbalanced and balanced datasets. Due to the small amount of fault samples in the imbalanced dataset, the model recognized 39 fault images as normal images. In a balanced dataset, as the fault samples increased, the recognition performance also significantly improved. When the fault samples were small, the training and learning effect was poor, and the monitoring effect of the equipment status was also reduced. In order to further analyze and study the performance of the designed model in the face of imbalanced datasets, the EDGAN model was used to perform data augmentation on a small number of samples in the imbalanced dataset. The accuracy of the model before and after data augmentation was compared, as shown in Figure 11.

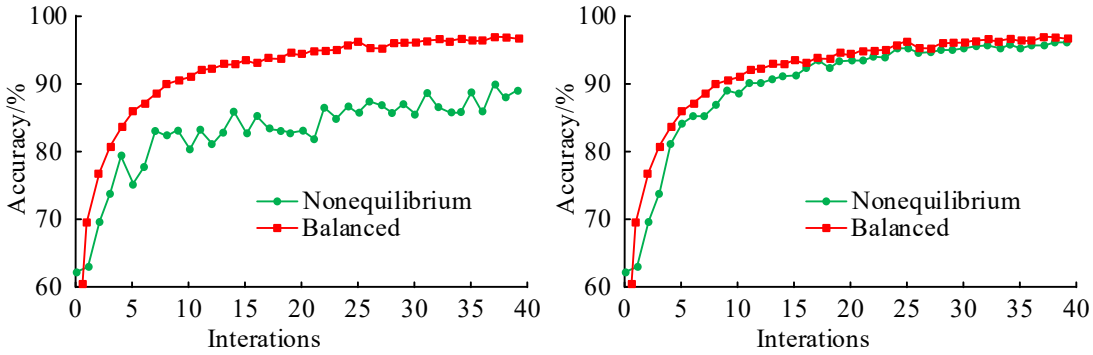

Figure 11. Comparison of model accuracy before and after data enhancement

Figure 11 (a) shows the model accuracy without data augmentation, and Figure 11 (b) shows the model accuracy after augmentation on an imbalanced dataset. It can be seen that after data augmentation, the accuracy of the model in imbalanced datasets can also be improved to around 96%. The use of EDGAN can enhance sample data and effectively improve model training effectiveness.

4.2. Analysis of practical application of the model

To further analyze the feasibility of the constructed electrical ESM model in practical application, IIG monitoring was carried out on the electrical equipment within the daily inspection scope of X City Power Supply Bureau. Figure 12 shows the detailed results.

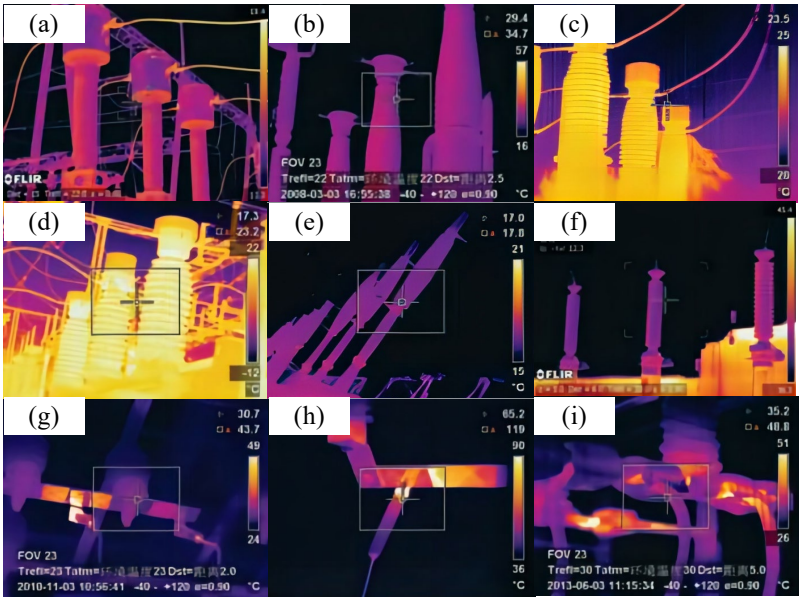

Figure 12. Status monitoring results of electric power equipment

Figures 12 (a) to (d) all show Normal: 100%. 12 (e) is Normal: 80%. 12 (f) is Normal: 95%. Figures 12 (g) to (i) show Warning: 100%. The research method could effectively compare the temperature distribution patterns under normal and abnormal conditions, thereby accurately identifying abnormal situations in equipment operation. Threshold method and clustering method were commonly used methods for image semantic segmentation. To further analyze whether the proposed model can enhance the semantic segmentation effect of electrical equipment image faults, a comparison was made between the threshold method, clustering method, and EDGAN model in image fault semantic segmentation based on fault detection. Figure 13 is a comparison chart.

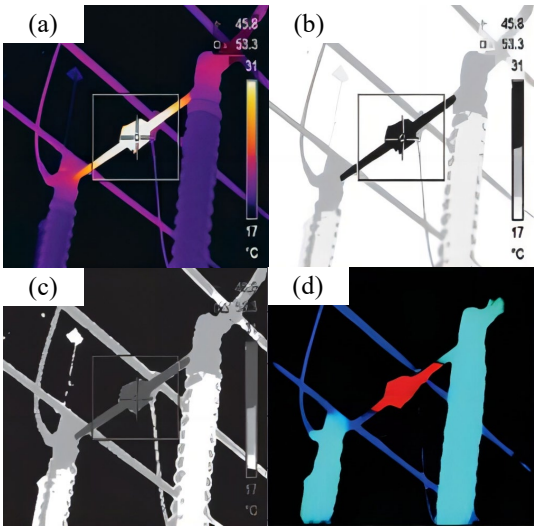

Figure 13. Fault image semantic segmentation results

Figure 13 (a) shows the original image. 13(b) to (d) show the segmentation result of the threshold, clustering method, and EDGAN methods. Compared to the other two semantic segmentation methods, the EDGAN model had better semantic segmentation performance. However, due to the presence of overlapping occluded parts in the image, some device edges were missing or incorrectly segmented.

5. Conclusion

This study aimed to construct a data mining-based rapid monitoring system for the status of power equipment to achieve real-time and accurate monitoring of O-PS status. The excellent performance of using EDGAN method had been demonstrated through the use of IFI data from daily inspections by X City Power Supply Bureau. Experiments had shown that the amplification of fault samples significantly improved classification accuracy and F1 score on existing imbalanced datasets, especially with the use of softmax classifier. The model's performance on balanced datasets was extremely stable, with a recognition accuracy of 96%. The balanced dataset generated through EDGAN could effectively lift the accuracy of fault identification and low-down false positives compared to the original imbalanced dataset. In practical application analysis, the model demonstrated excellent monitoring capabilities for the operation status of power equipment, accurately identified normal and abnormal states, and proposed preventive measures. The constructed electrical ESM model can effectively achieve electrical ESM and provide equipment fault alarms. The construction of this model can enhance the stable O-PS and ensure the safety of electricity consumption for residents. However, the training effect of this model on imbalanced datasets is poor. In the future, the training process of the model can be further optimized to enhance its learning ability and improve its robustness.

Reference

[1] Lee S B, Stone G C, Antonino-Daviu J, Gyftakis K N, Strangas E G, Maussion P, Platero C A. Condition monitoring of industrial electric machines: State of the art and future challenges. IEEE Industrial Electronics Magazine, 2020, 14(4): 158-167.

[2] Lu S, Chai H, Sahoo A, Phung B T. Condition monitoring based on partial discharge diagnostics using machine learning methods: A comprehensive state-of-the-art review. IEEE Transactions on Dielectrics and Electrical Insulation, 2020, 27(6): 1861-1888.

[3] Gui J, Sun Z, Wen Y, Tao D, Ye J. A review on generative adversarial networks: Algorithms, theory, and applications. IEEE Transactions on Knowledge and Data Engineering, 2021, 35(4): 3313-3332.

[4] Jiang T, Li Y, Xie W, Du Q. Discriminative reconstruction constrained generative adversarial network for hyperspectral anomaly detection. IEEE Transactions on Geoscience and Remote Sensing, 2020, 58(7): 4666-4679.

[5] Gao Y, Gao L, Li X. A generative adversarial network based deep learning method for low-quality defect image reconstruction and recognition. IEEE Transactions on Industrial Informatics, 2020, 17(5): 3231-3240.

[6] Gao Y, Gao L, Li X. A generative adversarial network based deep learning method for low-quality defect image reconstruction and recognition. IEEE Transactions on Industrial Informatics, 2020, 17(5): 3231-3240.

[7] Jin X, Xu Z, Qiao W. Condition monitoring of wind turbine generators using SCADA data analysis. IEEE Transactions on Sustainable Energy, 2020, 12(1): 202-210.

[8] Zhao Z, Davari P, Lu W, Wang H, Blaabjerg F. An overview of condition monitoring techniques for capacitors in DC-link applications. IEEE Transactions on Power Electronics, 2020, 36(4): 3692-3716.

[9] Di Lorenzo G, Araneo R, Mitolo M, Niccolai A, Grimaccia F. Review of O&M practices in PV plants: Failures, solutions, remote control, and monitoring tools. IEEE Journal of Photovoltaics, 2020, 10(4): 914-926.
[10] Wang B, Dong M, Ren M, Wu Z, Guo C, Zhuang T, Xie J. Automatic fault diagnosis of infrared insulator images based on image instance segmentation and temperature analysis. IEEE Transactions on Instrumentation and Measurement, 2020, 69(8): 5345-5355.
[11] Liu M Y, Huang X, Yu J, Wang T C, Mallya A. Generative adversarial networks for image and video synthesis: Algorithms and applications. Proceedings of the IEEE, 2021, 109(5): 839-862.
[12] Maeda H, Kashiyama T, Sekimoto Y, Seto T, Omata H. Generative adversarial network for road damage detection. Computer-Aided Civil and Infrastructure Engineering, 2021, 36(1): 47-60.
[13] Pavan Kumar M R, Jayagopal P. Generative adversarial networks: a survey on applications and challenges. International Journal of Multimedia Information Retrieval, 2021, 10(1): 1-24.
[14] Zhao B, Wang C, Fu Q, Han Z. A novel pattern for infrared small target detection with generative adversarial network. IEEE Transactions on Geoscience and Remote Sensing, 2020, 59(5): 4481-4492.
[15] Jiang Y, Chen H, Loew M, Ko H. COVID-19 CT image synthesis with a conditional generative adversarial network. IEEE Journal of Biomedical and Health Informatics, 2020, 25(2): 441-452.
[16] Souibgui M A, Kessentini Y. De-gan: A conditional generative adversarial network for document enhancement. IEEE Transactions on Pattern Analysis and Machine Intelligence, 2020, 44(3): 1180-1191.
[17] Souibgui M A, Kessentini Y. De-gan: A conditional generative adversarial network for document enhancement. IEEE Transactions on Pattern Analysis and Machine Intelligence, 2020, 44(3): 1180-1191.
[18] Daihong J, Sai Z, Lei D, Yueming D. Multi-scale generative adversarial network for image super-resolution. Soft Computing, 2022, 26(8): 3631-3641.
[19] Shi Y, Davaslioglu K, Sagduyu Y E. Generative adversarial network in the air: Deep adversarial learning for wireless signal spoofing. IEEE Transactions on Cognitive Communications and Networking, 2020, 7(1): 294-303.
[20] Hasanvand M, Nooshyar M, Moharamkhani E, Selyari A. Machine Learning Methodology for Identifying Vehicles Using Image Processing. AIA, 2023, 1(3): 170-178.